J Mater Sci (2006) 41:6708–6717
DOI 10.1007/s10853-006-0184-7

Composites reinforced with single crystalline oxide fibres: experiments and modelling

S. T. Mileiko

Published online: 8 August 2006

Abstract Metal- and ceramic-based composites reinforced with single crystalline oxide fibres promise an essential advance in developing heat-resistant composites. However, to reach a goal of making composites, which would be high creep resistant at very high temperatures and sufficiently damage tolerant at room temperature, a number of scientific and technological problems must be solved. The paper focuses on a particular feature of metal- and oxide-matrix composites, which is an interaction between fibre and matrix yielding considerable changes in microstructure and effective properties of both constituents. A special attention is drawn to a possibility to organize a synergetic fibre/matrix interaction to obtain composites with really new properties.

Introduction

The aim of the present paper is to answer two main questions:

1. Why composites reinforced with single crystalline oxide fibres should be considered as a primary topic for advanced composite science?
2. What are correlations between theory (modelling) and experiments with metal-matrix composites (MMCs)?

The answer to the first question is rather obvious and it has three aspects, namely the *necessity, present possibilities*, and *complicity of the problem*.

S. T. Mileiko (✉)
Solid State Physics Institute of Russian Academy of Sciences, Chernogolovka, Moscow distr 142432, Russia
e-mail: mileiko@issp.ac.ru

The *necessity* of high-temperature composites is determined by a need to increase use temperature of structural materials to increase thermal efficiency of machines and to decrease a load on the Earth and Biosphere. Increasing the effective temperature of the thermodynamic cycle yields also a decrease in a total volume of exhausts, which cause the air pollution.

The *present possibilities* are determined by availability of such fibres. A principal possibility to produce sapphire fibres has been known from the early days of modern composite materials, the Edge-Feed-Growth (EFG) method invented by LaBelle and Mlavsky [1] is actually a variation of a more general concept of crystal growth with the use of a shaper suggested by a Russian called Stepanov before the Second World War and published only in Russian after WWII. However, the EFG method applied to oxide fibres is characterized by a low productivity rate and, hence, yields high quality fibres of a cost too high to use them in structural materials. This made the present author to develop an alternative method to produce single crystalline fibres as reinforcement for structural composites. The fundamentals of a new method were developed in the Soviet times; the first papers disclosed a scheme of the method [2, 3] were published in early 90s. The method is called the internal crystallisation method (ICM) since the fibres are crystallised in continuous cylindrical channels pre-made in a molybdenum matrix. The recent review of the ICM can be found elsewhere [4]. However, to realize the possibilities, a number of scientific and technological problems must be solved: the complicity of the problem is perhaps a highest in the material science.

The *complicity of the problem* of high-temperature composites is determined by a number of the reasons; non- stability of the microstructure, which limits the use temperature of all heat-resistant materials, is perhaps most important one.

In the present paper, composites with metal and oxide matrices will be considered. We start with a brief description of the fibres, then discuss in some detail a special feature of the behaviour of a typical MMCs with non-oxide fibres, which provides an instructive example of an affect of the fibre on the matrix microstructure. Finally, modelling creep behaviour of oxide-fibre composites reveals ways of the influence of the interface and matrix on effective properties of the fibre. The cases to be considered show clearly that the constituents properties in a composites can differ essentially from their properties determined in separate testings.

To point out an importance of modelling the mechanical behaviour of high-temperature composites we present here a recent result in the developing oxide-fibre/brittle matrix composites of high damage tolerance, which has been achieved by constructing a special microstructure of the composites. Original load/displacement curves for specimens with single-crystalline oxide fibres and brittle matrices are shown Fig. 1. Non-brittle behaviour of composites with brittle TiAl-based and alumina matrices is obvious. However, it is also obvious that the macrostructure needs to be optimising to enhance failure stress and to make composites with uni-directional reinforcement be stronger than those with random-in-plane reinforcement. The optimisation can be done provided an adequate modelling of the failure processes is established.

Single crystalline oxide fibres

Single crystalline fibres obtained by using the internal crystallisation method has some features that should be taken into account while modelling mechanical behaviour of the composites reinforced with them. Those features are:

1. At present, they have a rather unusual shape of the cross section illustrated in Fig. 2.
2. They are characterised by a strong scale dependence, an example is presented in Fig. 3.
3. Coating a fibre with different materials by using CVD process yields an essential increase in the fibre strength; see also an example in Fig. 3.

An important property of a fibre to be reinforcements for heat-resistant composites is creep resistance. That characteristic of ICM-fibres obtained in molybdenum matrix is measured by testing oxide-fibre/molybdenum-matrix composites in bending [5]. An interpretation of the test results to obtain tensile creep characteristics of the fibre is based on an appropriate creep model, which is discussed below, in Sect. ''Creep of oxide-fibre/molybdenum-matrix specimens in bending''. Here just final results of the interpretation are presented in Fig. 4.

A strength model of MMCs

A strength model of MMCs developed by the present author long time ago [8] will be briefly described here focusing on a problem of modelling the strength behaviour of MMCs and, in particular, on an influence of the fibre on matrix properties.

At low fibre volume fractions, a fibre fails accumulating breaks without interactions with neighbouring fibres. The

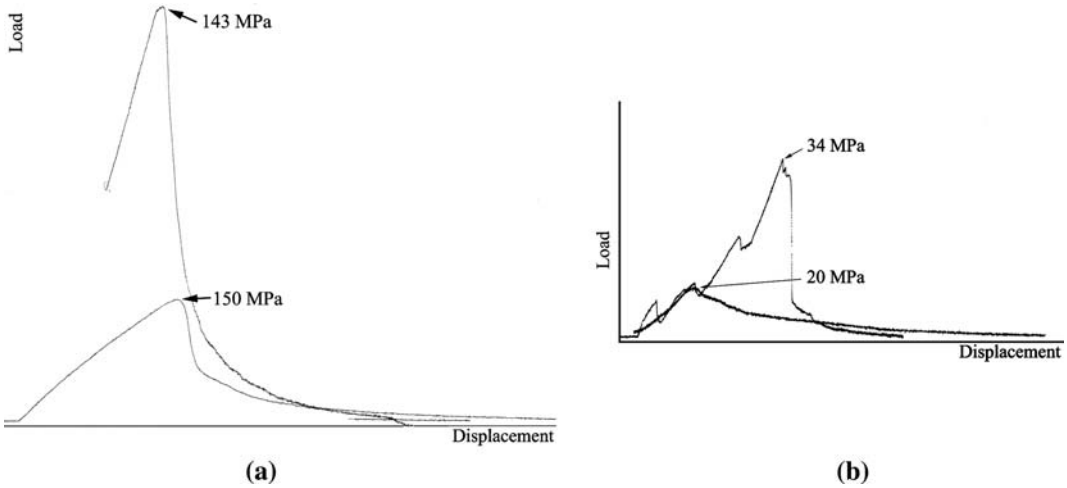

Fig. 1 Load vs. displacement for 3-point bending of oxide-fibre/brittle-matrix composites with a special microstructure at room temperature. (**a**) TiAl-matrix composite specimens. The matrix fails in a brittle manner at the ultimate stress between 420 and 500 MPa. (**b**) Alumina-matrix composites specimens at room temperature. The specimen with maximum flexure stress σ_{max} = 20 MPa has a unidirectional reinforcement, that with σ_{max} = 34 MPa has a random-in-plane reinforcement

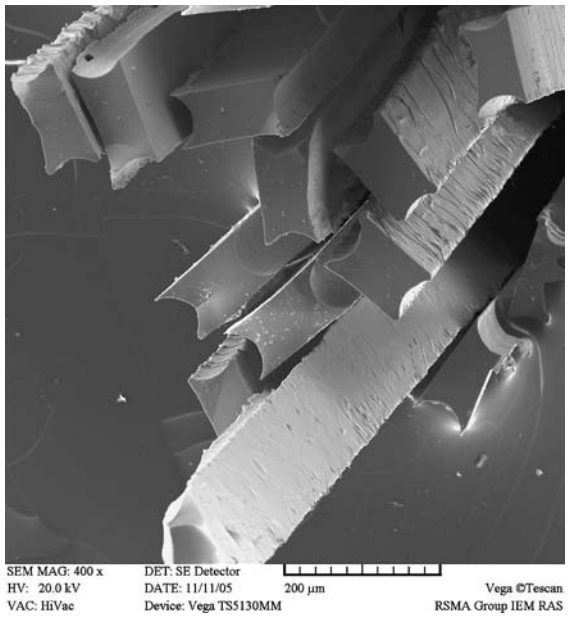

Fig. 2 Garnet fibres obtained by using the internal crystallisation method

dependence of the mean strength of a composite on fibre volume fraction will be

$$\sigma^* = \gamma\sigma_{\mathrm{f}}^*(l^*)V_{\mathrm{f}} + \sigma_{\mathrm{m}}^* V_{\mathrm{m}} \tag{1}$$

where $\sigma_{\mathrm{f}}^*(l^*)$ is the mean fibre strength on length l^*, l^* is the average distance between fibre breaks, σ_{m}^* is the matrix strength, γ is a constant. The corresponding dependence is depicted schematically in Fig. 5.

At large fibre volume fractions, a fibre/fibre interaction should not be neglected. It yields to a necessity to take into account the non-homogeneity of fibre packing, an exaggerated example of which is given on a real micrograph of a boron/aluminium specimen presented in Fig. 5. Consider a simplified situation when fibres are combined in linear bundles or clusters composed of n fibres. Such bundles have characteristic size nd, d being the fibre diameter. A crack with length $c \geq d$ is unstable within a bundle; if a microcrack arises at a fibre defect it grows up to size nd.

A first fibre break leading to a microcrack with length equal to nd happens when the mean composite strength reaches, on average, value

$$\langle\sigma_n^*\rangle = \langle\sigma_{\mathrm{f}}^*(L)\rangle V_{\mathrm{f}} + \sigma_{\mathrm{m}}^* V_{\mathrm{m}} \tag{2}$$

where L is a total fibre length in a composite, σ_{m}^* is the ultimate strength of the matrix material. A crack appeared is stable if

$$\langle\sigma_n^*\rangle$$

where σ^* is the Orowan's stress that is in the present case

$$\sigma^* = \sqrt{\frac{CG}{\lambda nd}}. \tag{3}$$

Here C is a known function of the components of the tensor of elastic moduli. G is the energy release rate of the composite, which can be written as

$$G = \begin{cases} G_{\mathrm{m}}^{\mathrm{o}}(1 - V_{\mathrm{f}}) & \text{at } V_{\mathrm{f}} < V_{\mathrm{f}}^{\mathrm{o}} \\ G_{\mathrm{m}}^{\mathrm{o}} \frac{V_{\mathrm{m}}^2}{V_{\mathrm{f}}} \frac{d}{h_{\mathrm{m}}} & \text{at } V_{\mathrm{f}} \geq V_{\mathrm{f}}^{\mathrm{o}} \end{cases}.$$

Here

$$G_{\mathrm{m}}^{\mathrm{o}} = \sigma_{\mathrm{m}}^* \varepsilon_{\mathrm{m}}^* h_{\mathrm{m}}$$

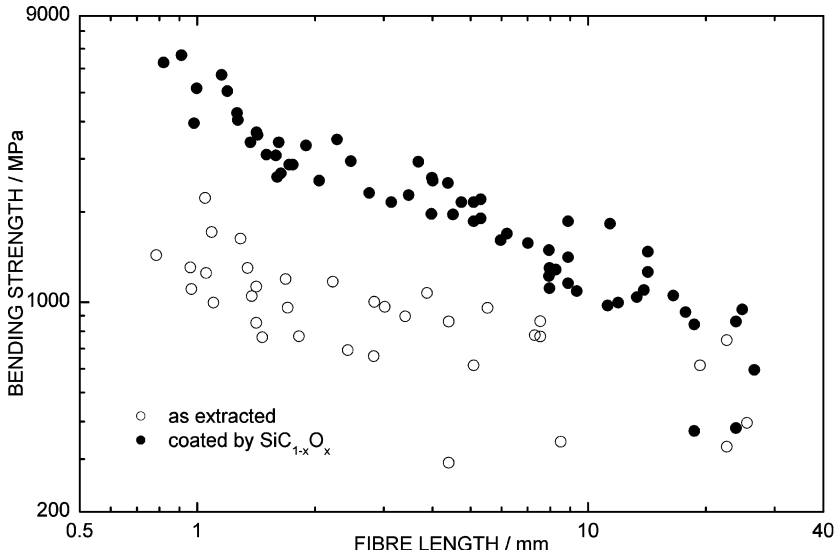

Fig. 3 Bending strength of a batch of sapphire fibre vs. fibre length. The strength was measured by looping up a fibre around a series of rigid cylinders of a decreasing length

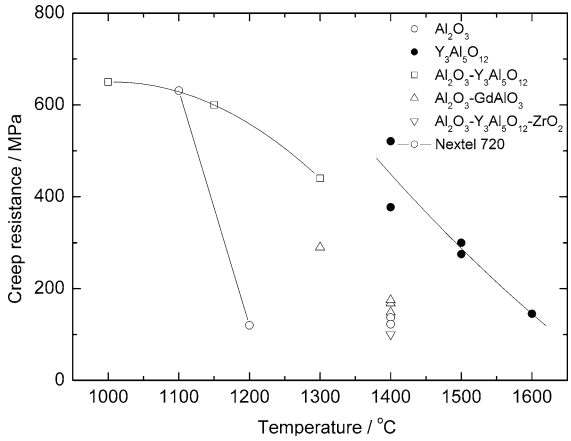

Fig. 4 Creep resistance (tensile stress to cause 1% creep strain for 100 h) of some single crystalline and eutectic oxide fibres produced by using the ICM [3, 6] in comparison with that of polycrystalline mullite-based fibre Nextel-720 (after [7])

where $\varepsilon_{\mathrm{m}}^{*}$ is the ultimate strain of the matrix material, h_{m} is a characteristic size,

$$V_{\mathrm{f}}^{\mathrm{o}} = \frac{1}{1 + h_{\mathrm{m}}/d}.$$

The line corresponding to Eq. (3) is depicted schematically in Fig. 5. The intersection of this line with that given by Eq. (1) at point A determines critical value V_{f}^{*} of fibre volume fraction, which separates two regimes of composite failure. The second one, at $V_{\mathrm{f}} > V_{\mathrm{f}}^{*}$, is actually failure at a weakest link: a specimen fails as soon as a microcrack arises. Hence, the strength/fibre-volume-fraction dependence follows line OAB until the line corresponding to Eq. (2) meets that given by Eq. (3), which is not shown in Fig. 5 as it is not important in the present context.

Comparing the model prediction with experimental data (see Fig. 6, open points) carried out on specimens with bad fibre packing shown in Fig. 5 yields, at least qualitatively, the expected result: the composite strength drops down at a quite low fibre volume fraction. However, the occurrence of the critical fibre volume fraction and, consequently, a drop in the composite strength for boron/aluminium composites with a nearly ideal fibre distribution in a specimen cross-section (Fig. 6, solid points) causes a question about a reason for it since no fibre bundles can be observed in this case. The answer was found while considering behaviour of boron in aluminium matrix alloyed with magnesium. It is known that solubility of boron in aluminium is negligible; so numerous studies of the microstructure of B/Al composites in early days of MMCs were focusing on formation of aluminium borides on the fibre/matrix interface and their influence on the effective fibre strength. Perhaps, the only exception was paper by Kim et al. [9] who drew attention to a thermodynamically based possibility of arising either magnesium borides or aluminium–magnesium borides provided Mg is present in an Al-based matrix, which is an actual case.

It was suggested [10] that heat treatment of the composites could yield a kind of pumping out boron by magnesium present in the matrix and cleaning off the matrix from boron by forming magnesium borides or/and aluminium–magnesium borides as inclusions in the matrix. The process, which can be described as internal boriding by analogy with well-known process of internal oxidation, is depicted schematically in Fig. 7. This yields formation of influence zones around boron fibres. The matrix in these zones is being strengthened and becoming brittle. Hence, arising such zones is accompanied by strengthening the composite until occurring critical brittle fibre clusters, which yield composite failure according to the dependence given by Eq. (3) even for composites that have no geometrical fibre bundles.

Despite the experimental case just considered is not that of a composite reinforced with oxide fibres, it has been

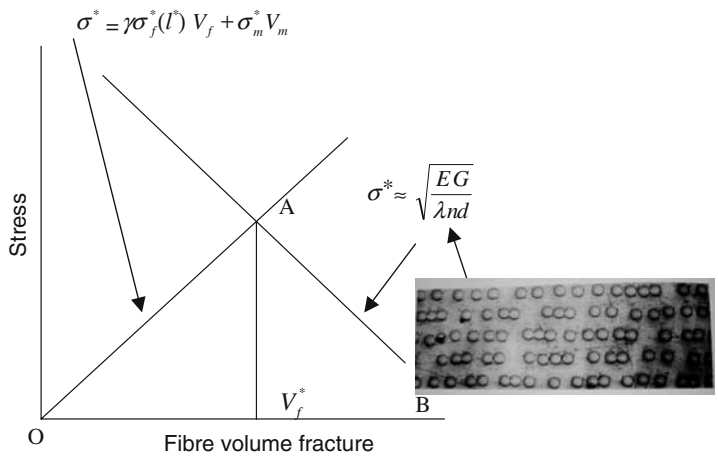

Fig. 5 Schematic presentation of the strength model of a MMC

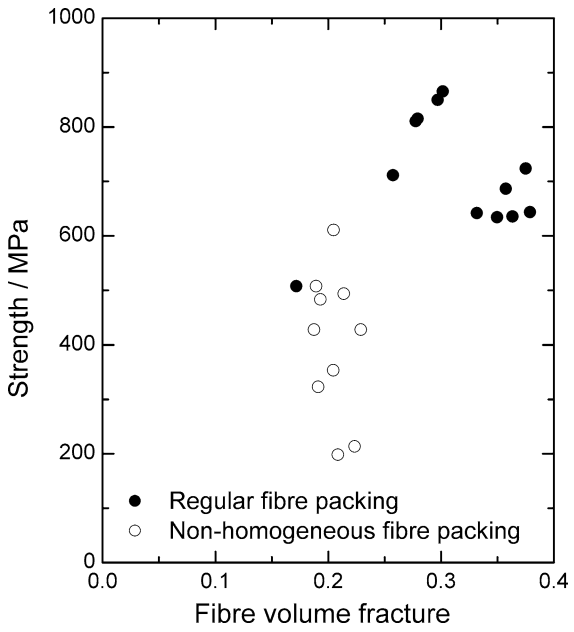

Fig. 6 Experimental dependencies of strength of a boron–aluminium composite with a regular fibre packing and non-homogeneous fibre packing presented on the micrograph in Fig. 5

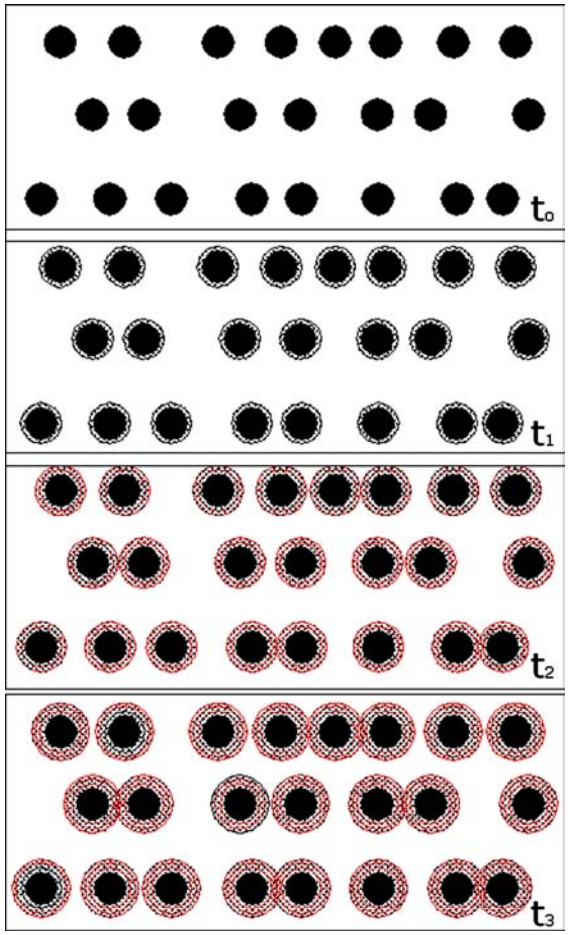

Fig. 7 Schematic of the growth of influence zones around boron fibres

discussed here since it represents an instructive example of an affect of the fibre on both the matrix properties and macrostructure of the composite as a whole.

Creep models of composites with creeping matrix

We consider a composite with creeping matrix and initially continuous fibres. A continuous fibre means that its length is much larger than a critical fibre length. Obviously, there can be observed at least four creep regimes of such composite:

1. **E**: Fibres are elastic and non-breaking.
2. **Br–NCr**: Fibres are elastic and brittle.
3. **Cr**: Fibres are creeping and non-breaking.
4. **Br–Cr**: Fibres are creeping and brittle.

Let the creep law of the matrix will be

$$\dot{\varepsilon} = \eta_{\mathrm{m}} \left(\frac{\sigma}{\sigma_{\mathrm{m}}} \right)^{m} \tag{4}$$

where η_{m}, σ_{m}, and m are constants, one of which can be chosen arbitrarily, so in what follows we take $\eta_{\mathrm{m}} = 10^{-4}$ h^{-1}.

For regime **E**, the dependence of fibre stress on time at a constant composite stress, σ, will obviously be

$$\sigma^{(\mathrm{f})}(t) = \frac{\sigma}{V_{\mathrm{f}}} \left\{ 1 - V_{\mathrm{m}} \left[\frac{V}{V_{\mathrm{m}} + \eta_{\mathrm{m}}(m-1)\frac{V_{\mathrm{f}}E_{\mathrm{f}}}{\sigma_{\mathrm{m}}} \left(\frac{\sigma}{\sigma_{\mathrm{m}}} \right)^{m-1} t} \right]^{\frac{1}{m-1}} \right\} \tag{5}$$

Here $V = V_{\mathrm{m}} + V_{\mathrm{f}}E_{\mathrm{f}}/E_{\mathrm{m}}$, where E_{f} and E_{m} are Young's moduli of the fibre and matrix, respectively, V_{f} and V_{m} are their volume fractions.

The creep strain of the composite is actually elastic deformation of the fibre changing with time

$$\varepsilon(t) = \frac{\sigma^{(\mathrm{f})}(t)}{E_{\mathrm{f}}}, \quad \varepsilon \to \frac{\sigma}{E_{\mathrm{f}}V_{\mathrm{f}}} \quad \text{at } t \to \infty. \tag{6}$$

A curve given by Eq. (6) is illustrated in Fig. 8.

For a composite with initially continuous brittle fibres creeping in regime **Br–NCr**, the dependence between creep rate and stress is written [5] as

$$\sigma = \lambda\sigma_{\mathrm{m}} \left[\left(\frac{\sigma_{\mathrm{o}}^{(\mathrm{f})}}{\lambda\sigma_{\mathrm{m}}} \right)^{\beta} \left(\frac{l_{\mathrm{o}}}{d} \right) \right]^{\frac{m+1}{q}} \left(\frac{\dot{\varepsilon}}{\eta_{\mathrm{m}}} \right)^{\frac{1}{q}} V_{\mathrm{f}} + \sigma_{\mathrm{m}} \left(\frac{\dot{\varepsilon}}{\eta_{\mathrm{m}}} \right)^{\frac{1}{m}} V_{\mathrm{m}} \tag{7}$$

where β is the exponent in the Weibull distribution for the fibre strength, $\sigma_{\mathrm{o}}^{(\mathrm{f})}$ is the average strength of a fibre of

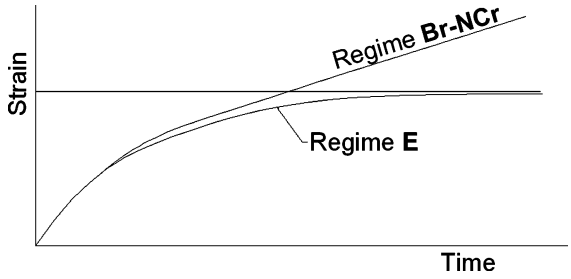

Fig. 8 Schematic creep curves for regimes **E** and **Br–NCr**

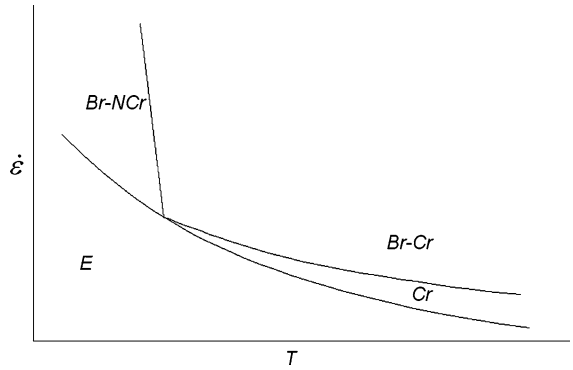

Fig. 9 A schematic map of the creep regimes of composites under homogeneous stress state

length l_o and characteristic cross-sectional size d, $q = m + \beta + m\beta$, and

$$\lambda = \alpha\left(\frac{2}{3}\right)^{\frac{1}{m}}\left(\frac{m}{2m+1}\right)\left[\left(\frac{2\sqrt{3}}{\pi}\right)^{-\frac{1}{2}} - 1\right]^{-\frac{1}{m}}.$$

An important parameter, α, is a continuity factor describing the fibre/matrix interface strength, $\alpha \to 0$ if there is no bonding at the interface, $\alpha = 1$ for an ideal bonding when the interface strength is equal to that of the matrix. Note that Eq. (7) was obtained assuming steady state creep followed the ending of the fibre breakage process on the transitional stage of creep. It occurs that the larger is α the shorter is the fibre length in the steady-state condition and, hence, the larger a stress carried by the fibre. An illustration of the dependence is presented also in Fig. 8.

For regime **Cr**, creep-rate/stress dependence is obvious:

$$\sigma = \sigma_f\left(\frac{\dot{\varepsilon}}{\eta_f}\right)^{\frac{1}{n}} V_f + \sigma_m\left(\frac{\dot{\varepsilon}}{\eta_m}\right)^{\frac{1}{m}} V_m \tag{8}$$

where η_f, σ_f, and n are constants in a power low for the fibre similar to Eq. (4).

Regime **Br–Cr** is a combination of regimes the two ones just described.

Schematic of all creep regimes can be presented as a map shown in Fig. 9. Exact boundaries between the particular areas can be traced by using both calculation and experiments.

Oxide-fibre/metal-matrix composites

As mentioned above, creep characteristics of ICM-fibres were normally obtained by testing specimens of composites with molybdenum matrix in bending. Here we are to describe briefly the procedure of interpreting the experimental results and then discuss in more details the behaviour of Ni-based composites.

Creep of oxide-fibre/molybdenum-matrix specimens in bending

When the whole specimen creeps in regime **E**, there are no special problems in interpreting the experimental results. An example of a creep curve obtained in such case is presented in Fig. 10. Note that displacements at the specimen centre shown in this figure and all following figures were measured in such a way that initial portion of the creep curves included bearings of supports and the specimen in a contact zone, so it cannot be used to evaluate fibre characteristics. Note also that small jumps on the curves are artefacts and do not reflect any special features of creep behaviour of the specimen.

While a most stressed volume of a specimen occurs to be in regime **Cr** (Fig. 9), a schematic example is shown in Fig. 11a, then a boundary between regions **Cr** and **E** is moving with time enlarging the **Cr**-region. The neutral axis is obviously also moving towards region **E**. A steady-state creep, which is characteristic for regime **Cr** in the case of a homogeneous stress state, cannot be reached. However, a nearly constant displacement rate of a specimen is observed as shown in Fig. 12 (specimen V0729). This means that a main contribution to the displacement is conveyed by region **Cr** and the results obtained can be used to calculate a first approximation to tensile creep characteristics of the fibres. The fundamentals of the interpretation procedures is outlined in Ref. [5], particular procedures used to evaluate creep characteristics of the fibres are presented in V.M. Kiiko and S.T. Mileiko (submitted). It should be noted that, as a rule, specimens were tested at a step-wise loading to evaluate value of the exponent in the accepted power law of creep for a particular specimen.

On the other hand, if a test starts with a sufficiently large load and at the beginning of the test a part of the specimen occurs to be in regime **Br–Cr** (Fig. 11b) then the situation changes drastically. Regions of three regimes occur and

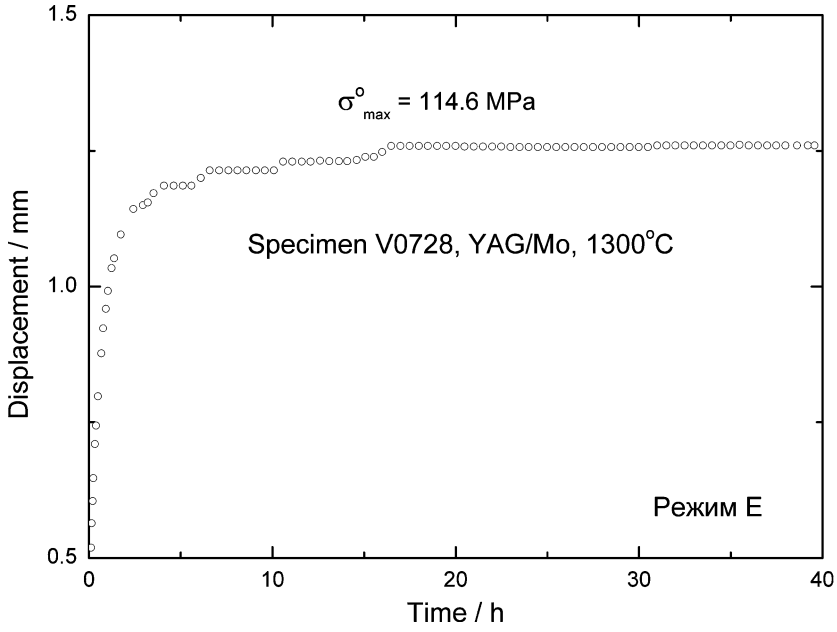

Fig. 10 A flexture creep curve of YAG-fibre/molybdenum-matrix composite. The whole specimen creeps certainly in regime **E**. The value of maximum elastic stress is shown in the field

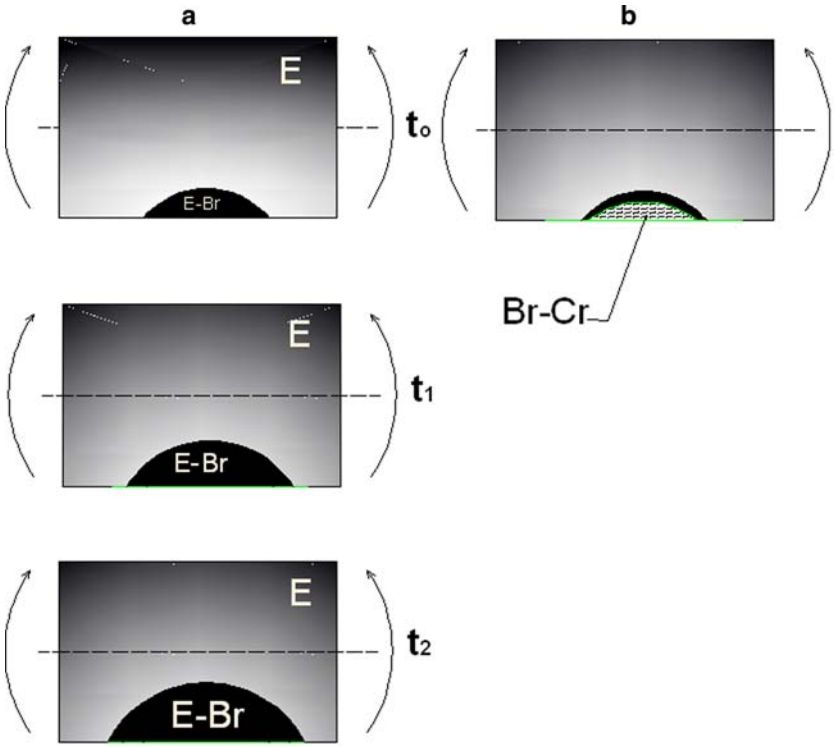

Fig. 11 A schematic of moving a boundary between volumes of a specimen that creeps under 3-point bending conditions

displacement rate can be higher by orders of magnitudes then in the case when regime **Br–Cr** is avoided as a result of redistribution of the macro-stresses under smaller applied loads. The difference is seen when comparing displacement rates at the same values of the load for two similar specimens in Fig. 12.

It should be noted that the boundaries in the map depicted in Fig. 9 are drawn schematically, constructing the exact map requires calculations based on experimental data and creep models. Also it is important to note that the creep characteristics of oxide fibres presented in Fig. 4 have been obtained by interpreting experimental data on

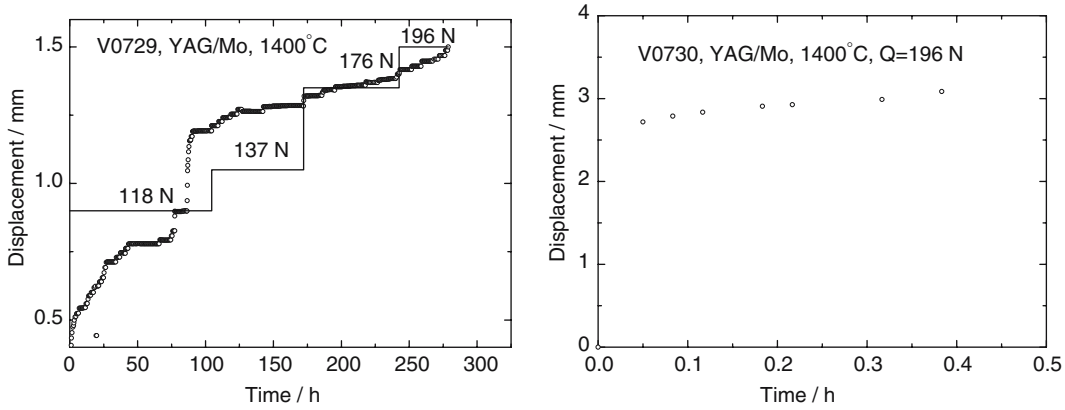

Fig. 12 Flexture creep curves of two YAG-fibre/molybdenum-matrix composite specimens of about the same sizes (see Table 1)

flexure creep of oxide/molybdenum composites on the basis of Eq. (7). That means that regime **Br–Cr** is assumed to be observed within the whole volume of a specimen but not only in the volume making a large contribution to the displacement.

Oxide-fibre/nickel-based matrix composites

Most important experimental results illustrating a correlation between the creep resistance of composites and interface strength that determines the composite creep resistance according to Eq. (7) are presented in Fig. 13. The creep resistance has been measured by testing the specimens in bending; interface strength has been measured by using a modified push-out technique [11]. It can be seen that the average interface strength deceases essentially at fibre volume fraction above 25%. This corresponds to a decrease in the creep resistance: the stress/fibre-volume-fraction curve deviates clearly from an extrapolation of the stress/fibre-volume-fraction dependence observed at low fibre volume fractions (Fig. 13).

Equation (7) describes the creep behaviour of composites with large fibre volume fractions and a weak matrix/matrix interface, $\tau^* \approx 20$ MPa ($\alpha = 0.01$), when accepting a value of the fibre strength equal to 150 MPa, which is characteristic value for fibres tested separately.

To describe the behaviour of the composites at low fibre volume fractions (strong interface), we need, obviously, to increase the value of α. However, increasing only the value of α does not yield a satisfactory result; to make the dependences for various α to be consistence with the experimental points, it is necessary to assume variations of the fibre strength characteristics together with variations of the interface strength. Such assumption is not an artificial procedure. The first experimental fact supporting an idea of the fibre strength characteristics being affected the interface microstructure is an observation of strengthening the fibre as a result of coating the fibre with a layer of sufficiently rigid material, see Fig. 3; more experimental data of the same type can be found in Ref. [12]. Secondly, TEM-observations of the microstructure of the interface [13] reveal just a partial contact on the matrix/matrix

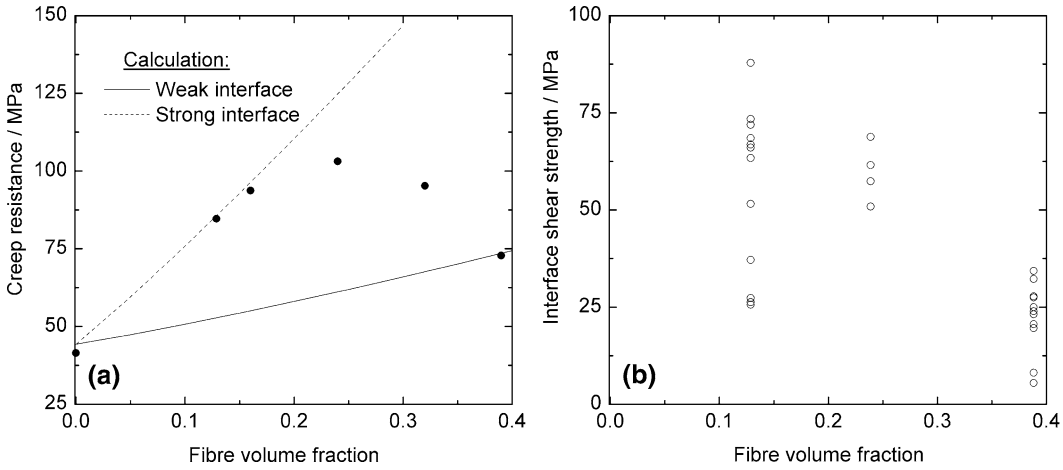

Fig. 13 Alumina-YAG-eutectic-matrix/Ni-based-matrix composites: (**a**) Stress to cause 1% creep strain for 100 h at 1150 °C vs. fibre volume fraction. (**b**) The interface strength vs. fibre volume fraction

Table 1 Parameters of the specimens mentioned in the paper

Specimen number	Fibre volume fraction	Specimen geometry		
		Height (mm)	Width (mm)	Distance between supports (mm)
V0728	0.36	4.2	4.45	54
V0729	0.45	4.3	4.15	54
V0730	0.36	4.25	4.4	54

interface in these composites. It should be noted that the stronger the interface, the larger portion of the fibre surface is in contact with the matrix. A continuous interface was observed in the Mo-based composite.

Hence, modelling creep, and perhaps, strength behaviour of the MMC one sometimes needs to take into account an affect of the fibre/matrix interface on the fibre strength characteristics. From the practical point of view, it is important to organise the interface in such a manner as to take advantage of a possibility to strengthen the fibre as a result of the fibre/matrix interaction. Moreover, the composites with high interface strength are an example of a synergetic system. Increasing the interface strength yield increasing the effective fibre strength in two ways, one being a classical scale effect due to decreasing the fibre critical length, and another one is an effect described for the first time in Ref. [5]: higher interface strength can be determined by a better interface microstructure, which yields healing fibre surface defects and further enhancing the fibre strength.

Creep of oxide-fibre/oxide-matrix composites

Here results of the experimental study of creep behaviour of uni-directional model composites with sapphire fibre and alumina matrix with a ''weak'' interphase formed by a layer of carbon. It was shown previously [14] that such microstructure is characterised by enhanced fracture toughness as compared to that of the matrix. In the preliminary series of creep experiments with such composites at 1,200 °C [A.A. Kolchin et al. submitted] it was found that their creep behaviour could be described by Eqs. (6) and (7). The calculated dependence of the creep resistance (stress to cause 1% creep strain for 100 h) on fibre volume fraction is presented in Fig. 14. The experimental data for four specimens tested are given in Table 2, typical microstructure of the composites are presented in Fig. 15. Specimen A2053 is characterised by extremely non-homogeneous fibre packing, it causes a decrease in the

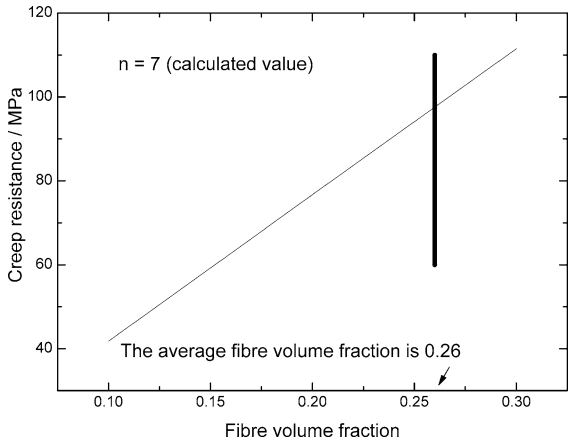

Fig. 14 The calculated creep resistance of sapphire-fibre/alumina-matrix composites at 1200 °C

Table 2 Experimental creep characteristics of sapphire-fibre/alumina-matrix composite specimens

Specimen number	n	Creep resistance (MPa)
A2005	6.01	94.9
A2007	5.60	77.8
A2034	5	64.3[a]
A2053	2.85	38.1

[a]The value was determined by using one step of loading and accepting $n = 5$

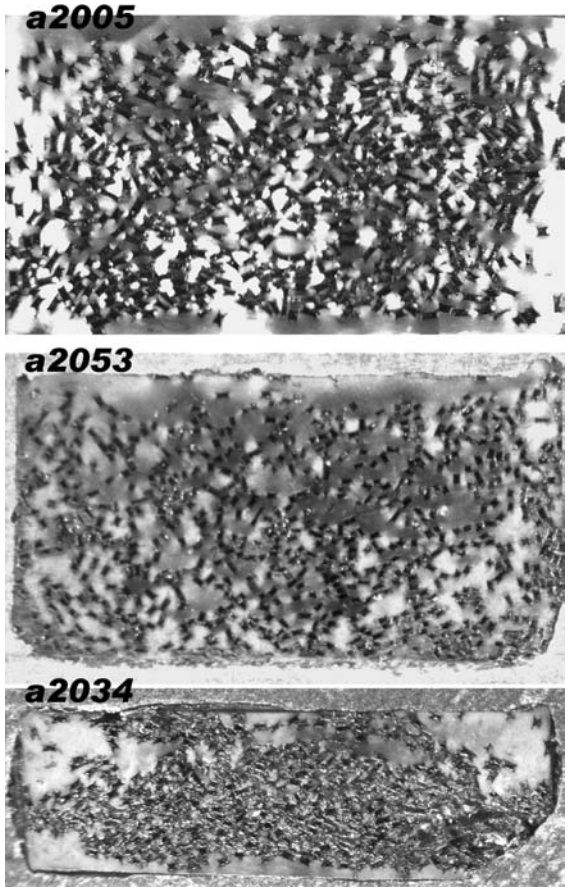

Fig. 15 Macrostructure of some sapphire/alumina specimens

creep resistance. It should be noted that the effective creep properties of the matrix occur to be quite moderate.

Conclusions

1. Single-crystalline oxide fibres now available in the form characteristic for the internal crystallisation method are suitable for the usage as reinforcements for composites with high use temperatures.
2. Comparing experimental results and model calculations is not a trivial procedure since the behaviour of a fibre and matrix tested separately and their behaviour in a composite can be different.
3. This calls for the development of a quantitative model of a fibre/matrix interaction of a deeper level than that now available.
4. A good composite is that behaving in a synergistic nature.

Acknowledgements The work was partly supported by International Science and Technology Centre, Project #2456, and Russian Foundation for Basic Research, Projects 04-03-81030-bÞeπ2004 and 05-08-50101. Former and present staff of Laboratory of Reinforced Systems of Solid State Physics Institute participated in the experimental work. Special thanks to A. Serebryakov, V. Kiiko, A. Kolchin, L. Kozhevnikov, V. Korzhov, V. Kurlov, I. Maleev, A. Mizkevich, N. Prokopenko, N. Sarkissyan.

References

1. LaBelle HE Jr, Mlavsky AI (1967) Nature 216:574
2. Mileiko ST, Kazmin VI (1992) J Mater Sci 27:2165
3. Mileiko ST, Kazmin VI (1992) Compos Sci Technol 45:209
4. Mileiko ST (2005) Compos Sci Technol 65:2500
5. Mileiko ST (2002) Compos Sci Technol 62:195
6. Mileiko ST, Kolchin AA, Kurlov VN, Kiiko VM, Serebryakov AV, Tolstun AN, Korzov VP, Novokhatskaya NI (2005) CD-Proceedings of 15th international conference on composite materials, Durban, South Africa, June 2005
7. Wilson DM, Visser LR (2001) Composites Part A 32:1143
8. Mileiko ST (1997) Metal and ceramic based composites. Elsevier, Amsterdam, p 235
9. Kim WH, Koczak MJ, Lawly A (1978) In: Noton B et al (eds) Proceedings of the 1978 international conference on composite materials, Toronto, April. Met. Soc. of AIME, New York, 1978, p 487
10. Mileiko ST, Sarkissyan NS, Serebryakov AV, Trifonov SV (1994) Compos Sci Technol 50:423
11. Prokopenko VM, Mileiko ST (2001) Compos Sci Technol 61:1649
12. Mileiko ST, Kiiko VM, Sarkissyan NS, Starostin MYu, Gvozdeva SI, Kolchin AA, Strukova GK (1999) Compos Sci Technol 59:1763
13. Mileiko ST, Kiiko VM, Kolchin AA, Serebryakov AV, Korzhov VP, Starostin MYu, Sarkissyan NS (2002) Compos Sci Technol 62:167
14. Kolchin AA, Kiiko VM, Sarkissyan NS, Mileiko ST (2001) Compos Sci Technol 61:1079